PNAS

Supporting Information for
Impact of Specific Electromagnetic Radiation on Wakefulness in Mice.

Hu Deng[1,2,5], Lingyu Liu[1,5], Xiaping Tang[3,4], Yingxian Lu[1], Xiaofei Wang[1 4], Yanyu Zhao[3,4], and Yigong Shi[1,3,4,*]

1 Beijing Advanced Innovation Center for Structural Biology & Frontier Research Center for Biological Structure, Tsinghua-Peking Joint Center for Life Sciences, School of Life Sciences, Tsinghua University, Beijing 100084, China;

2 Peking University Huilongguan Clinical Medical School, Beijing Huilongguan Hospital, Beijing 100096, China;

3Westlake Laboratory of Life Sciences and Biomedicine; 4 Key Laboratory of Structural Biology of Zhejiang Province, School of Life Sciences, Westlake University; Institute of Biology, Westlake Institute for Advanced Study, Shilongshan Road, Hangzhou 310024, Zhejiang Province, China;

5 These authors contributed equally to this work.

Corresponding author: Yigong Shi
E-mail: syg@westlake.edu.cn

This PDF file includes:

Supporting text
Figures S1 to S7
SI References

Supporting Information Text

Radiation equipment setup

2.4 GHz and 935 MHz EMRs are generated by a MXG Vector signal generator (Agilent, N5181A) modulated by a function generator (Rflight, NTWPA-1025100). The three modulation frequencies are 1000 Hz, 100 Hz, and 10 Hz, each of which is presented in squared or sinusoidal mode. Specific customized power amplifier was used to amplify different signal carriers of 2.4 GHz or 935 MHz to a maximal power output of 64 Watts. The EMR signal in parallel direction was emitted from a horn antenna (HD-26SGAH20NZJ). To minimize reflection of the electromagnetic wave, absorbing materials were fixed to the inside wall and floor of the animal container. We regularly check the peak power density that enters the horn antenna using a spectrum analyzer (Rigol, DSA875). For the Pulse64W regimen, the radiation level was maintained at 48±1 dBm, 48±1 dBm, and 48±1 dBm for the modulation frequencies of 10 Hz, 100 Hz, and 1000 Hz, respectively. We also checked the power densities in the mouse cage using an electromagnetic field meter (Wavecontrol S.L. SMP2 with WPF18 probe). The average noise level in the recording chamber was monitored using a digital sound level meter (Smart sensor, AS824). Over the course of 5 minutes, the average noise level was 67.3±0.36 dB for the control and 67.8±0.21 dB for the radiation group. Control and radiation mice were housed in the same environment and treated identically except for EMR exposure. The radiation mice were treated with EMR on days 1–9 (24 hours a day).

Animals

All animal protocols applied in this study have been approved by the Animal Care and Use Committee of Tsinghua University. Animal experiments were accredited and whole-process monitored by the Association for Assessment and Accreditation of Laboratory Animal Care International at Tsinghua University. All adult C57BL/6 wild-type male mice of 6-10 weeks were purchased from the Laboratory Animal Resources Center at Tsinghua University and housed in the specific pathogen free animal facility. The mice were maintained on a 12/12-hour light/dark cycle (ZT0: 10 a.m.), 22-26℃ with sterile pellet food and water ad libitum, and at least inhabited for 7 days before any treatment.

Electrode implantation

Mouse was anesthetized by intraperitoneal injection of avitine (300~375 mg/kg). Four cranial electrodes, each a stainless steel 304 screw (diameter 1.4 mm, length 4 mm), were secured to the skull. The two right electrodes (coordinates, bregma: AP +1.50 mm, ML +1.50 mm; AP -3.50 mm, ML +4.00 mm) were winded using silver wires as the reference or ground wires. EEG was recorded by wrapping a lacquered copper wire though the two left electrodes (coordinates, bregma: AP +1.50 mm, ML -1.50 mm; AP -3.50 mm, ML -3.00 mm) (1-3). The EMG electrode wires were embedded under the trapezius muscles in the neck of mouse. All electrodes and screws were attached to the skull with dental cement.

Polysomnographic recording and analysis

The EEG and EMG signals were collected via a digital head stage attached to the cranial electrodes. The data acquisition system receives digital signals with a sampling rate of 1000 Hz followed by signal filtration and amplification. All video signals were monitored. Relying on sleep analysis software, we analyzed the filtered EEG data (band-pass 0.5-100 Hz) using fast Fourier transformation (FFT). Relying on the spectral features of EEG, EMG, and acceleration signals, brain states were classified as wakefulness, NREM sleep, and REM sleep for every 4-second epoch (4).

Statistical analysis

The data are presented as the means ± standard error of the mean (SEM). The total time at Pre and Pos9 were compared between the control and the radiation groups using two-way repeated measures ANOVA with post-hoc comparisons (Bonferroni correction). The radiation effect index (REI) for each regimen was compared to 0 by one-sample t tests (two-tailed). The REIs of wakefulness and NREM sleep at Pos9 between different modulation frequencies for 2.4 GHz were compared using the ANOVA analysis. Because the REIPos9 values of REM sleep exhibit abnormal distribution, nonparametric test was used to compare the REIs at Pos9 of REM sleep between different modulation frequencies. All statistical analyses were conducted using Matlab and SPSS 20.0. Data visualization of raincloud plot was performed using Matlab modified from the open-source code (5).

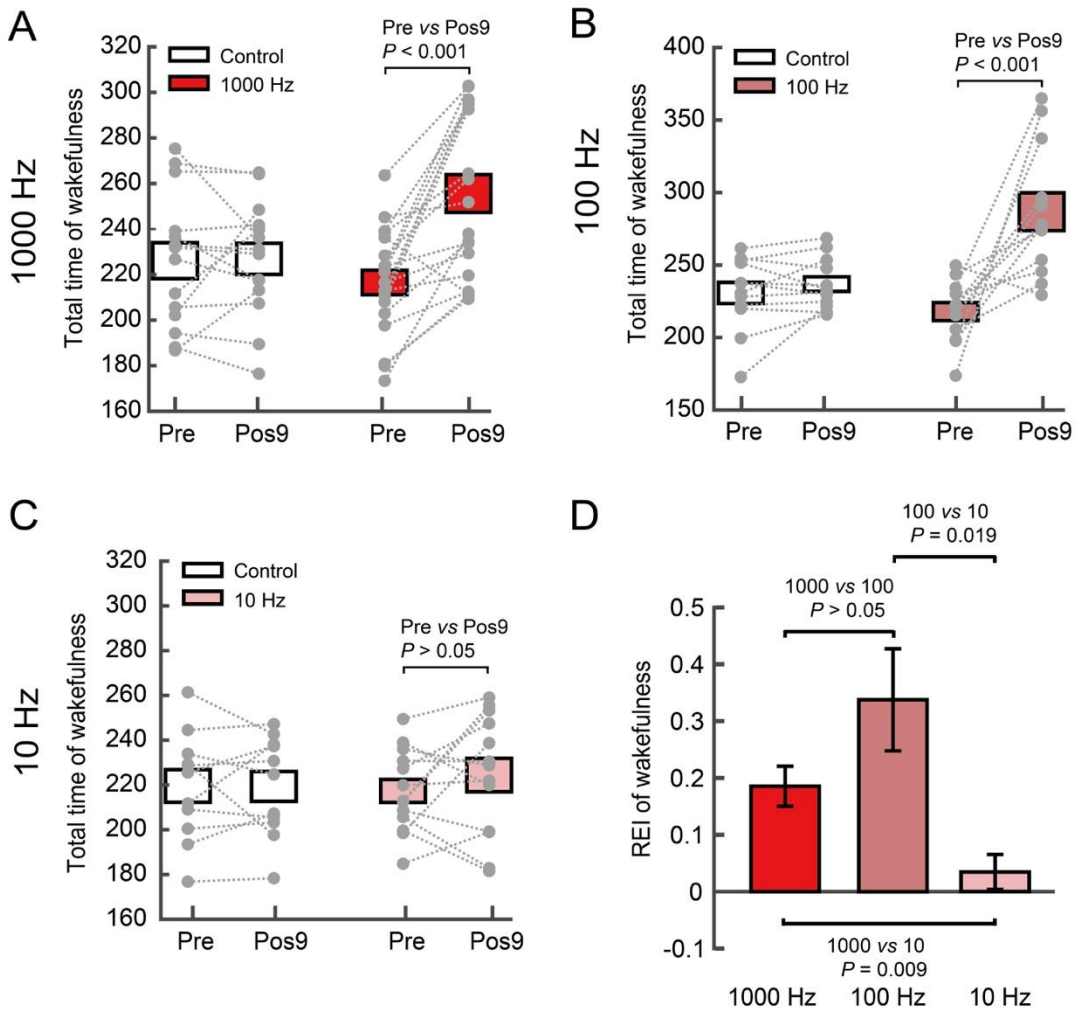


Fig. S1. The effect on wakefulness for the 2.4 GHz Pulse64W regimen with 1000 Hz, 100 Hz and 10 Hz modulation frequencies. (A) A scatter plot of wakefulness at Pre and Pos9 for mice exposed to 2.4 GHz Pulse64W EMR with a modulation frequency of 1000 Hz. Each dot represents the total time of wakefulness for individual mouse; the dotted line connects the data for the same mouse. (B) A scatter plot of wakefulness at Pre and Pos9 for mice exposed to 2.4 GHz Pulse64W EMR with a modulation frequency of 100 Hz. (C) A scatter plot of wakefulness at Pre and Pos9 for mice exposed to 2.4 GHz Pulse64W EMR with a modulation frequency of 10 Hz. (D) The comparison of REIPos9 values for wakefulness among 1000 Hz, 100 Hz, and 10 Hz square-pulsed modulations. This analysis shows statistically significant increases of wakefulness at Pos9 for 1000 Hz and 100 Hz modulations.

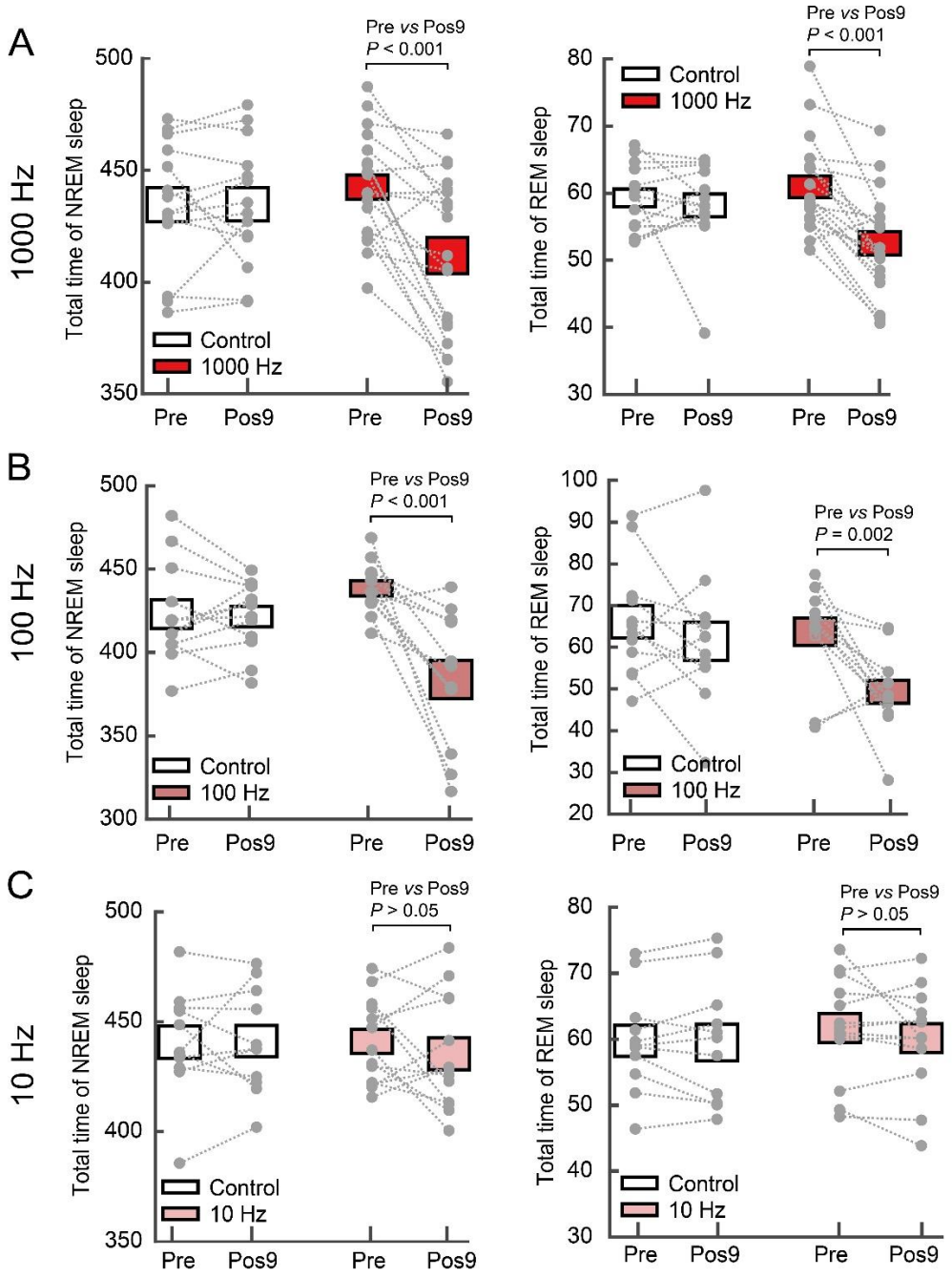


Fig. S2. The effect of the 2.4 GHz Pulse64W regimen on NREM sleep and REM sleep. (A) A scatter plot of NREM sleep (left panel) and REM sleep (right panel) at Pre and Pos9 for mice exposed to 2.4 GHz Pulse64W EMR with a modulation frequency of 1000 Hz. Each dot represents the total time of wakefulness for individual mouse; the dotted line connects the data for the same mouse. (B) A scatter plot of NREM sleep (left panel) and REM sleep (right panel) at Pre and Pos9 for mice exposed to 2.4 GHz Pulse64W EMR with a modulation frequency of 100 Hz. (C) A scatter plot of NREM sleep (left panel) and REM sleep (right panel) at Pre and Pos9 for mice exposed to 2.4 GHz Pulse64W EMR with a modulation frequency of 10 Hz.

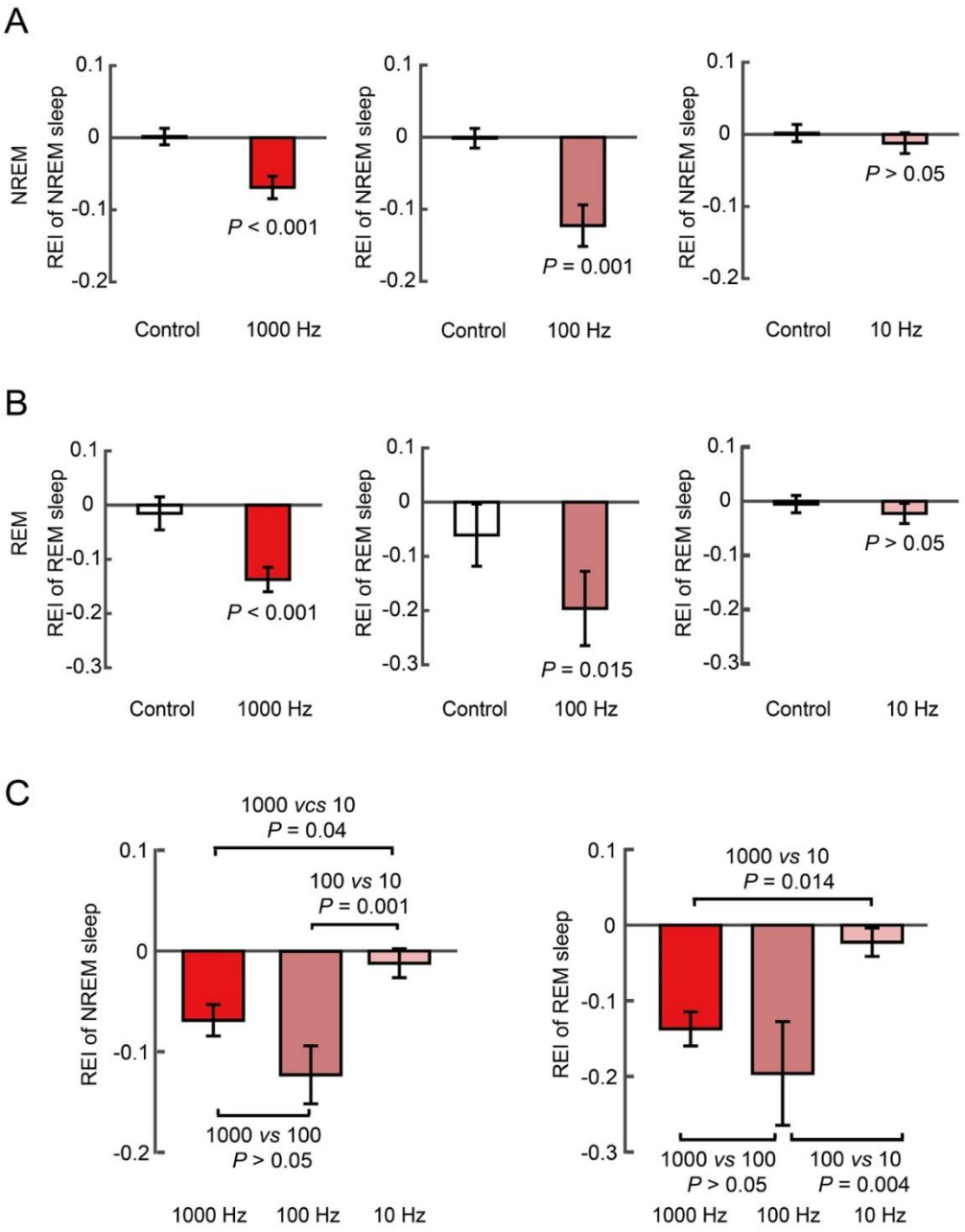


Fig. S3. REI analysis of the NREM sleep and REM sleep for mice exposed to the 2.4 GHz Pulse64W regimen modulated by three different frequencies. (A) The REIPos9 values of NREM sleep for the control and radiation groups exposed to 2.4 GHz Pulse64W EMR modulated by 1000 Hz (left panel), 100 Hz (middle panel), and 10 Hz (right panel). (B) The REIPos9 values of REM sleep for the control and radiation groups exposed to 2.4 GHz Pulse64W EMR modulated by 1000 Hz (left panel), 100 Hz (middle panel), and 10 Hz (right panel). (C) The comparison of REIPos9 values for NREM sleep (left panel) and REM sleep (right panel) among 1000 Hz, 100 Hz, and 10 Hz square-pulsed modulations.

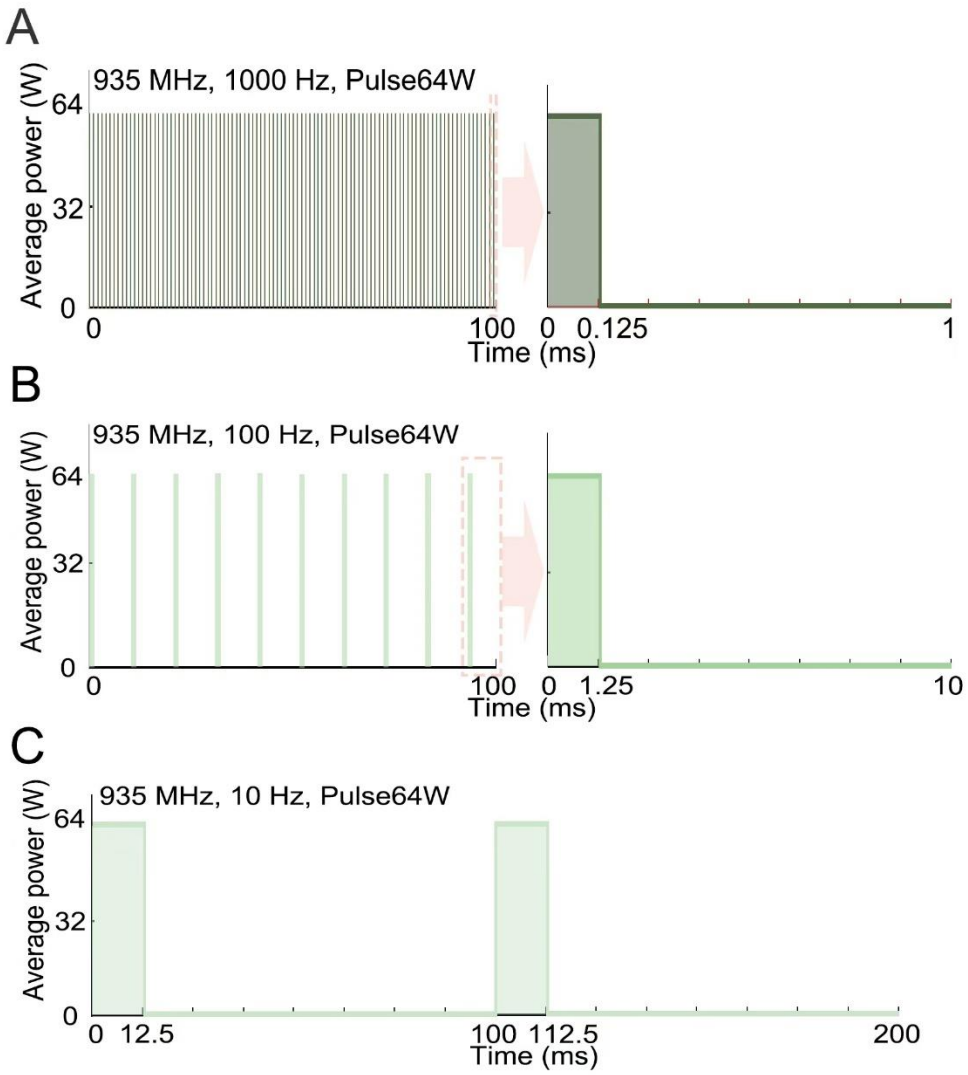


Fig. S4. Schematic diagrams of the 935 MHz Pulze64W EMR with three different modulation frequencies. (A) A schematic diagram of the 935 MHz Pulze64W EMR modulated by 1000 Hz square pulses at 1/8 duty cycle. 1000 Hz modulation: 1-millisecond (ms) repeats, each square pulse lasting 0.125 ms. (B) A schematic diagram of the 935 MHz Pulze64W EMR modulated by 100 Hz square pulses at 1/8 duty cycle. 100 Hz modulation: 10-ms repeats, each square pulse lasting 1.25 ms. (C) A schematic diagram of the 935 MHz Pulze64W EMR modulated by 10 Hz square pulses at 1/8 duty cycle. 10 Hz modulation: 100-ms repeats, each square pulse lasting 12.5 ms.

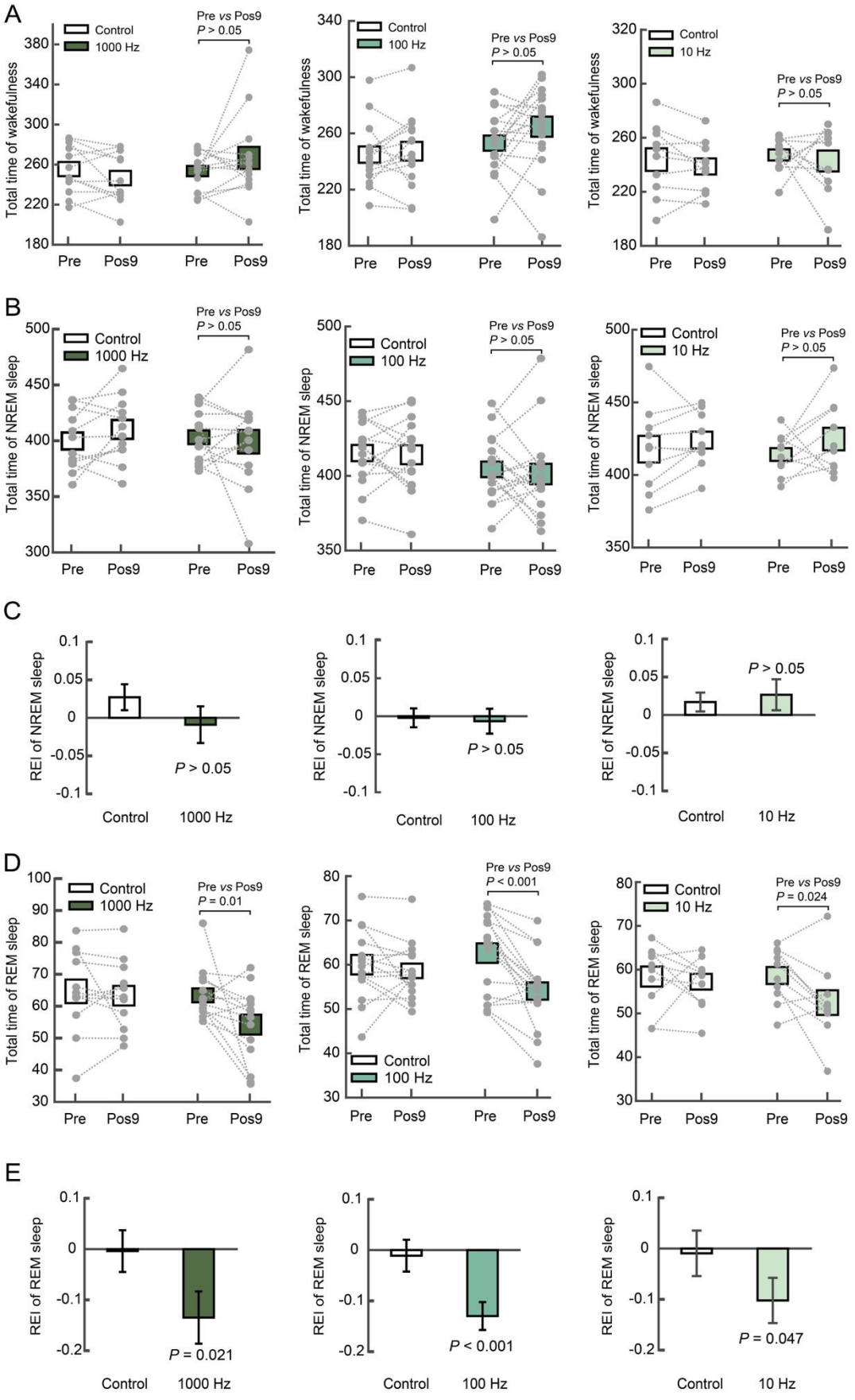

A
Control
1000 Hz
Pre vs Pos9
P > 0.05
Total time of wakefulness
Pre
Pos9
Control
100 Hz
Pre vs Pos9
P > 0.05
Total time of wakefulness
Control
10 Hz
Pre vs Pos9
P > 0.05
Total time of wakefulness
B
Control
1000 Hz
Pre vs Pos9
P > 0.05
Total time of NREM sleep
Control
100 Hz
Pre vs Pos9
P > 0.05
Total time of NREM sleep
Control
10 Hz
Pre vs Pos9
P > 0.05
Total time of NREM sleep
C
REI of NREM sleep
P > 0.05
Control
1000 Hz
REI of NREM sleep
P > 0.05
Control
100 Hz
REI of NREM sleep
P > 0.05
Control
10 Hz
D
Control
1000 Hz
Pre vs Pos9
P = 0.01
Total time of REM sleep
Control
100 Hz
Pre vs Pos9
P < 0.001
Total time of REM sleep
Control
10 Hz
Pre vs Pos9
P = 0.024
Total time of REM sleep
E
REI of REM sleep
P = 0.021
Control
1000 Hz
REI of REM sleep
P < 0.001
Control
100 Hz
REI of REM sleep
P = 0.047
Control
10 Hz

Fig. S5. The effect of the 935 MHz Pulse64W regimen on wakefulness, NREM sleep, and REM sleep. (A) A scatter plot of wakefulness at Pre and Pos9 for mice exposed to 935 MHz Pulse64W EMR with the modulation frequencies of 1000 Hz (left panel), 100 Hz (middle panel), and 10 Hz (right panel). Each dot represents the total time of wakefulness for individual mouse; the dotted line connects the data for the same mouse. (B) A scatter plot of NREM sleep at Pre and Pos9 for mice exposed to 935 MHz Pulse64W EMR with modulation frequencies of 1000 Hz (left panel), 100 Hz (middle panel), and 10 Hz (right panel). (C) The REIPos9 values of NREM sleep for the control and radiation groups exposed to 935 MHz Pulse64W EMR modulated by 1000 Hz (left panel), 100 Hz (middle panel), and 10 Hz (right panel). (D) A scatter plot of REM sleep at Pre and Pos9 for mice exposed to 935 MHz Pulse64W EMR with a modulation frequency of 1000 Hz (left panel), 100 Hz (middle panel), and 10 Hz (right panel). (E) The REIPos9 values of REM sleep for the control and radiation groups exposed to 935 MHz Pulse64W EMR modulated by 1000 Hz (left panel), 100 Hz (middle panel), and 10 Hz (right panel).

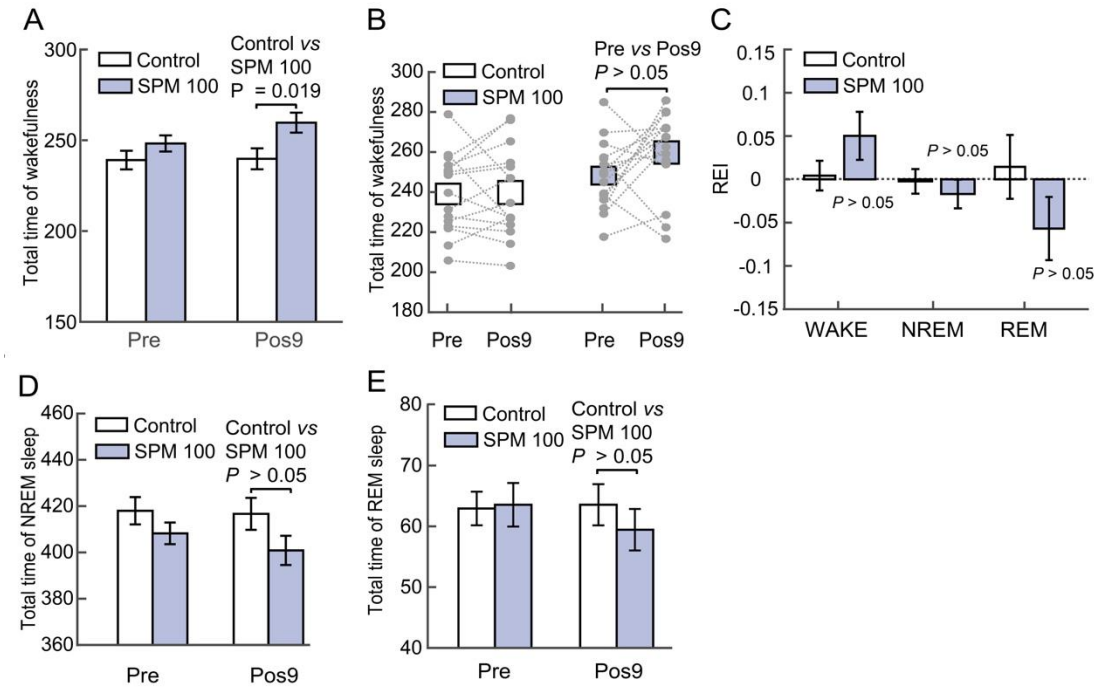


Fig. S6. Impact on sleep architecture by 935 MHz Pulse64W EMR with 100 Hz sinusoidal-pulsed modulation (SPM). (A) The 935 MHz Pulse64W regimen with 100 Hz SPM results in a moderate increase of wakefulness at Pos9 in mice. Shown here is the average time of wakefulness for the control and radiation groups at Pre and Pos9. n=15 for each group. (B) A scatter plot of wakefulness for total time of wakefulness of individual mouse. This analysis reveals a statistically insignificant change of wakefulness at Pos9, compared to Pre. (C) REI analysis of the change of sleep architecture. Shown here are the bar plots of REIPos9 values of wakefulness, NREM sleep and REM sleep. (D) The 935 MHz Pulse64W regimen with 100 Hz SPM results in a statistically insignificant change of the NREM sleep at Pos9 in mice. Shown here is the average time of NREM sleep for the control and radiation groups at Pre and Pos9. (E) The 935 MHz Pulse64W regimen with 100 Hz SPM results in a statistically insignificant change of the REM sleep at Pos9 in mice. Shown here is the average time of REM sleep for the control and radiation groups at Pre and Pos9.Type or paste legend here. Paste figure above the legend.

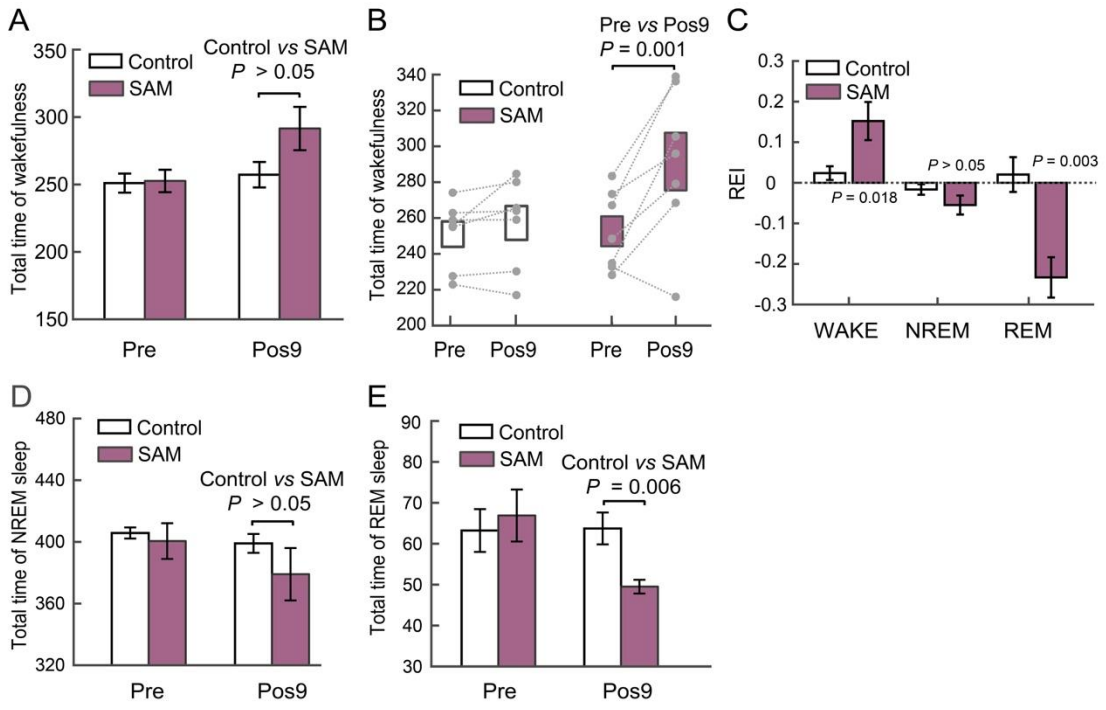


Fig. S7. Impact of 935 MHz 8W EMR with continuous sinusoidal amplitude modulation (SAM8W) on sleep architecture. (A) The 935 MHz SAM8W regimen results in a statistically insignificant increase of the wakefulness time at Pos9. Shown here is the average time of wakefulness for the control and radiation groups at Pre and Pos9. n=7 for each group. (B) A scatter plot of the wakefulness for the control and radiation groups. This analysis reveals a statistically significant increase of wakefulness at Pos9 compared to Pre for the radiation group. (C) Evaluation of the change of sleep architecture through REI analysis. Shown here are the bar plots of REIPos9 values of wakefulness, NREM sleep, and REM sleep for the radiation group. (D) The 935 MHz SAM8W regimen results in a statistically insignificant change of the NREM sleep at Pos9. Shown here is the average time of NREM sleep for the control and radiation groups at Pre and Pos9. (E) The 935 MHz SAM8W regimen results in a statistically significant decrease of the REM sleep at Pos9 in mice. Shown here is the average time of REM sleep for the control and radiation groups at Pre and Pos9.

SI References

1. Franklin K & Paxinos G (2008) The mouse brain in stereotaxic coordinates (Academic Press).
2. Xu M, et al. (2015) Basal forebrain circuit for sleep-wake control. *Nature Neuroscience* 18(11):1641-1647.
3. Chen K-S, et al. (2018) A Hypothalamic Switch for REM and Non-REM Sleep. *Neuron* 97(5):1168-1176.e1164.
4. Ren SC, et al. (2018) The paraventricular thalamus is a critical thalamic area for wakefulness. *Science* 362(6413):429-434.
5. Allen M, Poggiali D, Whitaker K, Marshall TR, & Kievit RA (2019) Raincloud plots: a multi-platform tool for robust data visualization. Wellcome open research 4:63.